https://doi.org/10.5194/egusphere-2025-1622
Preprint. Discussion started: 19 May 2025

Cyclone enhances the contribution of oceanic dimethyl sulfide to the free troposphere over the Southern Ocean

Miming Zhang *[1], Haipeng Gao[1], Shanshan Wang[1], Yue Jia[*2], Shibo Yan[1], Rong Tian[1], Jinpei Yan[1], Yanfang Wu[3]

[1] Key Laboratory of Global Change and Marine-Atmospheric Chemistry of Ministry of Natural Resources (MNR), Third Institute of Oceanography, MNR, Siming District, Xiamen, Fujian 361005, PR China
[2] School of Natural Sciences and Mathematics, University of Texas at Dallas, USA
[3] Department of Chemistry, University of Otago, Dunedin 9016, New Zealand

Correspondence to: Miming zhang (zhangmiming@tio.org.cn); Yue Jia (yue.jia@utdallas.edu)

Abstract. Under cold and clean atmospheric conditions, such as in free troposphere, oceanic dimethyl sulfide (DMS) was likely to form new particles. This is likely to happen over the Southern Ocean, where high DMS emissions occur along with frequent cyclones and storm activities which enhance vertical entrainment. Herein, the DMS contribution to free troposphere from the surface ocean was evaluated using the data collected from 34th Chinese Antarctic Research Expedition and Lana DMS emission climatology by running the Lagrangian particle dispersion model FLEXPART. Up to 13.1% of the DMS was found to be transported to the free troposphere (altitudes above 2 km) from the surface ocean, which was enhanced by the cyclones. High DMS mixing ratios (> 100 pptv) were found surrounding the cyclones even at an altitude of 5 km. These results indicate that the significant DMS-derived new particles have probably occurred in high altitudes of the Southern Ocean.

1 Introduction

It is well known that cloud condensation nuclei (CCN) can affect cloud formation, thus affecting the Earth's radiation budget (Rosenfeld et al. 2014; Dusek et al. 2006). Dimethyl sulfide (DMS), a critical oceanic short-lived gas (Liss et al. 2014), was proposed to strongly influence the CCN population in the marine boundary layer (MBL) and regulate global climate change (The CLAW hypothesis) (Charlson et al. 1987). However, this hypothesis was refuted (Quinn and Bates 2011) and, instead, they proposed that the CCN concentration in the remote MBL is mainly controlled by sea salt and organics in sea spray, subsidence of DMS-derived and continental derived particulates from the free troposphere, and particle growth. In addition, there is still uncertainty related to the formation of non-sea-salt sulfate (NSS) aerosol in the free troposphere from marine DMS emission (Quinn et al. 2017).

Several studies have corroborated that the entrainment of NSS particles from the free troposphere into MBL could be an essential factor driving the MBL CCN budget (Clarke et al. 2013; Raes 1995; Merikanto et al. 2009). Two main processes may

https://doi.org/10.5194/egusphere-2025-1622
Preprint. Discussion started: 19 May 2025

be responsible for forming NSS particles in the free troposphere: 1) DMS oxidation in the free troposphere. DMS may enter the free troposphere via buoyancy-driven vertical transport and be oxidized for nucleation in the cold free troposphere with few pre-existing particles (Sanchez et al. 2018); 2) Long-range transportation (LRT) of continental sulfur compounds from biomass burning or volcanic eruptions. For example, during the Pacific Atmospheric Sulfur Experiment (PASE), the observed entrainment of NSS to MBL mainly originated from LRT (Simpson et al. 2014). As NSS from the free troposphere is thought to be an important source of CCN to the MBL (Quinn and Bates 2011), investigating the sources of NSS in the free troposphere is warranted.

The Southern Ocean (SO) atmosphere is considered one of the most unpolluted global ocean regions, where aerosol is unlikely to be affected by either anthropogenic or natural continental sources (Ayers and Gillett 2000; Quinn et al. 1998). Aerosols over the SO mainly originate from primary wind-produced sea spray and secondary sulfate (gas-to-particle) formation (Murphy et al. 1998; McCoy et al. 2015). Additionally, the SO has been found to be a significant source of DMS (Kettle et al. 1999; Lana et al. 2011), and high seawater DMS concentrations, up to hundreds of nM, were observed in coastal waters (Tortell et al. 2012; Tortell et al. 2011; Tortell and Long 2009; Kim et al. 2017) and marginal sea ice areas (Zhang et al. 2017; Curran, Jones, and Burton 1998; Inomata et al. 2006). Therefore, DMS emitted over the SO could significantly influence the sulfate aerosols and the particle formation there. Previous studies indicated that CCN concentrations and seasonal variability are influenced, primarily, by biogenic DMS emission over the SO (Simó, and Gassó 2006; Gabric et al. 2005). A recent study in the Arctic also demonstrated that DMS could directly impact new particle formation and growth of particles (Park et al. 2021). Thus, understanding how oceanic DMS influences sulfate aerosols and particle formation over the SO is essential.

Another interesting feature of the SO region is the frequent occurrence of cyclone and storm activities (Patoux et al., 2009). These meteorological phenomena not only impact the momentum and heat fluxes at the air-sea interface (Yuan et al., 2009), as well as ocean stratification (Plessis et al. 2019), but also enhance sea-to-air fluxes of trace gases in MBL due to high wind speeds (Nightingale et al. 2000), and their vertical transportation in the atmosphere (Marandino et al. 2013; Tegtmeier et al. 2013). Therefore, during SO cyclone events, it is possible that biogenic DMS emitted to MBL can be transported into the free troposphere.

Several cyclone events were encountered along the cruise track during the 34th Chinese Antarctic Research Expedition (CHINARE) (Zhang et al. 2019; Zhang et al. 2020). High-resolution (10 min) measurements of both surface seawater and lower atmospheric DMS were collected during this expedition. In this study, the Lagrangian particle dispersion model FLEXPART (Stohl et al. 2005) was used in combination with calculated DMS fluxes from the CHINARE expedition and those from the Lana DMS emissions climatology (Lana et al. 2011) to investigate the contribution of DMS entrained to the free troposphere from the MBL over the SO during major storm events.

https://doi.org/10.5194/egusphere-2025-1622
Preprint. Discussion started: 19 May 2025

2 Method and material

2.1 Ship measurements

Our measurements were performed on board the *R/V Xue Long* from February 23 to Mar 4, 2018, during CHINARE 34th (Figure 1 a). The shipboard underway measurements of atmospheric and seawater DMS were conducted using a custom-made automatic purge and trap system coupled with a time-of-flight mass spectrometer (TOF-MS, SPI-MS 3000, Guangzhou Hexin Instrument Co., Ltd., China) (Zhang et al. 2019). A pair consisting of one atmospheric and one seawater DMS data point can be recorded every 10 min with a detection limit of 0.07 nM and 36 pptv, respectively.

2.2 Calculation of DMS sea-to-air flux

The F_{DMS} is calculated by a widely used gas exchange model considering both the water-air side and air-water side as follows:

$$F = (1-A)\, k_w\, (1- \gamma_a)\, (C_w - C_g/H) \quad (1)$$

where A is the sea ice cover fraction; K_w is the gas transfer velocity using the empirical parameterization of (Nightingale et al. 2000). C_w and C_g are the seawater and atmospheric DMS concentrations, respectively. H is the Henry's law solubility coefficient (Dacey, Wakeham, and Howes 1984). The calculation of γ_a, indicating the partitioning between air-side and water-side control, is presented in equation (2) (McGillis et al. 2000).

$$\gamma_a = 1/(1+k_a/\alpha k_w) \quad (2)$$

A detailed description of k_a (air-side transfer coefficient) and α (Ostwald solubility coefficient) can be found in McGillis et al., (2000) and the references therein.

2.3 Modelling

The Lagrangian particle dispersion model (FLEXPART) was selected to simulate the atmospheric distribution and transport of DMS (Stohl et al. 2005). This model has been previously validated through comprehensive comparisons with field measurements (Stohl et al., 1998; Stohl and Trickl 1999). FLEXPART operates by calculating the trajectories of numerous of so - called particles (small air parcels) to describe the transport, diffusion, and chemical decay of tracers in the atmosphere. The model takes into account turbulence in the boundary layer and free troposphere (Stohl and Thomson 1999) and features a moist convection scheme (Forster et al., 2007) that follows the parameterization proposed by Emanuel and Živković - Rothman (1999). To account for the chemical or radioactive decay of the transported tracer, the model reduces the tracer mass in the air parcels according to the tracer's prescribed lifetime.

For this study, we used FLEXPART version 10.0. This version was driven by 3 - hourly meteorological fields sourced from the ECMWF (European Centre for Medium - Range Weather Forecasts) reanalysis product ERA - Interim (Dee et al. 2011).

https://doi.org/10.5194/egusphere-2025-1622
Preprint. Discussion started: 19 May 2025

The horizontal resolution of these fields is 1° x 1°, and there are 61 vertical model levels. The total study area covered is 3.25 × 10^7 km^2. For all simulation runs in high-latitude regions, a lifetime of 2 days was specified for DMS (Read et al. 2008). The simulations were carried out for the period of the campaigns, with each run having a 1 - week spin - up period. Specifically, the simulations were run from Feb 18, 2018, to Mar 10, 2018, to ensure a stable background concentration in the atmosphere.

3.0 Results and discussion

3.1 The DMS source and air mass dynamics

As shown in our previous study (Zhang et al. 2020), a large-scale area with high seawater and atmospheric DMS concentrations was found outside the Ross Sea sector of the SO during the campaign, with maximum values up to 27.9 nmol L^{-1} and 3.92 ppbv, respectively. The calculated DMS sea-to-air fluxes, with peaks up to 27.5 μmol m^{-2} d^{-1}, are presented in Figure 1 a. Clearly, the strong DMS flux is associated with the observed DMS hotspot (above 10 nM). It is noteworthy that the negative DMS values occurred when considering the atmospheric DMS in the flux calculation, which could be explained by the accumulation of high atmospheric DMS values in regions with low seawater DMS concentration due to atmospheric transport (Zhang et al. 2020). Additionally, our calculated DMS flux is lower than Lana's climatology (Lana et al. 2011) along the cruise track.

During the campaign, cyclones were encountered along the cruise track, which is indicated by low air pressure (< 970 hPa, Figure 1 c) (marked with red arrows). The ice-free SO is known as a region with frequent cyclone activity, especially in the Amundsen and Bellingshausen Seas (Irving et al., 2010). Coincidentally, the large-scale DMS hot spot detected during the campaign was located close to the southern cyclone, suggesting that the cyclone event had the potential to enhance both the sea-to-air exchange of DMS through high wind speeds and the vertical transport from the MBL to free troposphere. To understand the influence of low-pressure systems on the vertical transport of oceanic DMS, it is necessary to investigate air mass dynamics.

The height of plume centroids and the corresponding mean mixing height of each time step during the simulation period are presented (Figure 1 b, d). Generally, the mean mixing heights are below 1.0 km except those in the relatively small areas between 50°S and 60°S, ranging from 1.0 km to 1.25 km. According to the results plume centroids' heights are generally higher than the mean mixing heights of corresponding time steps, indicating that the vertical transportation of air masses capacity, partially enhanced by the cyclones, seems strong enough to break through the MBL to the free troposphere. Subsequently, the oceanic trace gases could possibly be transported to high altitudes through detrainment.

https://doi.org/10.5194/egusphere-2025-1622
Preprint. Discussion started: 19 May 2025

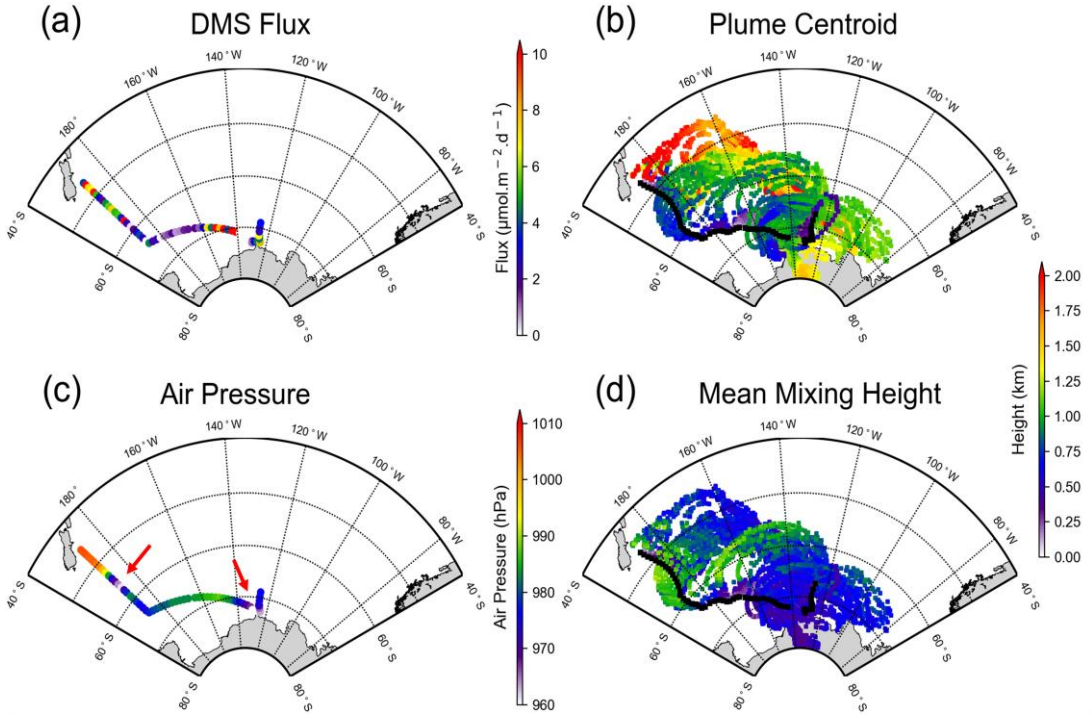

Figure 1. DMS sources and air mass dynamics along the cruise track during the cruise period. a) DMS flux, b) plume centroids, c) air pressure, note that red arrows indicate the low-pressure systems, and d) mean mixing height. Transect (black line) during the expedition from Feb 23 to Mar 4, 2018. A lifetime of 2 days forward trajectories are prescribed during all runs.

3.2 Modelling the DMS distributions at different altitudes over the SO

To understand how marine-derived DMS is transported through the atmosphere, we first investigate the mean modelling results based on the DMS flux data estimated from the cruise track area (assumed as a continuous 1º × 1º point). The spatial distribution of atmospheric DMS at different altitudes indicates that the DMS emitted from the cruise track could be transported to a large-scale area, and the DMS mixing ratios generally decreased with height (Figure 2 a, b, c). However, when we compare results across regions with similar DMS flux values (Figure 1 a), we generally see that the regions with high atmospheric DMS levels are found surrounding a low-pressure core. Additionally, peaks of atmospheric DMS are located near the low-pressure core near 140°W at 3 km and 5 km respectively (Figure 2 b, c), suggesting that under a low-pressure system, the marine-derived DMS could be transported upward to higher altitudes, even to the free troposphere. The strong influence of low-pressure systems on the vertical transport of oceanic DMS is supported further by the negative relationship between the integrated mean vertical distributions of atmospheric DMS peaks and 500 hPa geopotential height during the investigation period (Figure 2, d).

https://doi.org/10.5194/egusphere-2025-1622
Preprint. Discussion started: 19 May 2025

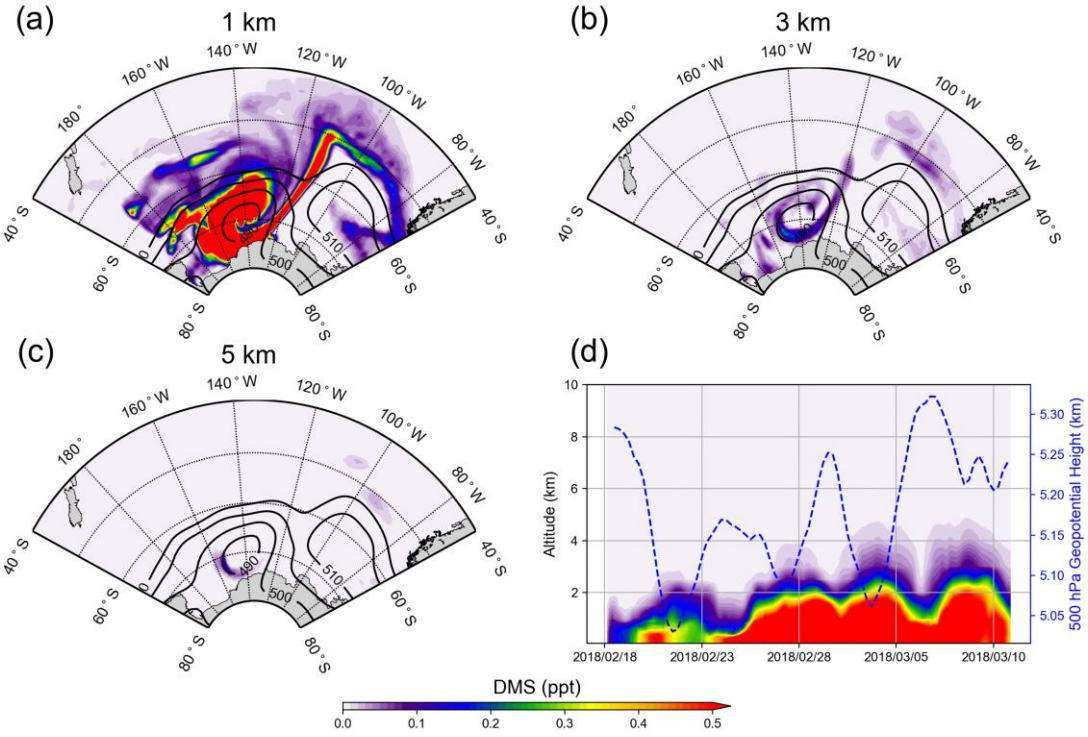

Figure 2, Modelling results of mean DMS distributions at different altitudes using the CHINARE campaign data. Mean distributions of atmospheric DMS at altitudes of **a)** 1 km, **b)** 3 km and **c)** 5 km. Note that the mean 500 hPa geopotential air pressures are presented in the background. **d)** The variations of average vertical distributions of atmospheric DMS associated with the changes of mean 500 hPa geopotential height.

To analyze the relationship between the vertical transport of DMS and low-pressure systems in detail, we present the daily variation of DMS spatial distribution over the SO at different altitudes (Figure S1 - S3 for 1 km, 3 km, and 5 km, respectively) from the simulation based on the CHINARE campaign. As seen in Figure S2, the atmospheric DMS mixing ratios are quite low (generally < 0.2 ppt), but peaks can still be found near the low-pressure systems (cyclones or troughs). For example, a peak of about 0.2 ppt appeared around 180°, 60°S on Feb 24th, 2018 (Figure S2 b), corresponding to the trough therein. In the following days, the peak, with a decreasing magnitude, moved eastward along the trough (Figure S2 c, d, e). Relatively high atmospheric DMS mixing ratios were also found around 140°W, 70°S on Mar 3rd, 2018, indicating the influence of the low-pressure core therein. Even at 5 km, the relatively high atmospheric DMS mixing ratios were simulated to occur around the troughs or low-pressure cores (Figure S3).

However, we could only indicate the ability of atmospheric transport of the DMS emitted from the shipping route from the CHINARE campaign. To fully understand the information of the atmospheric transport of the DMS emitted from the whole study area, simulations based on the well-known global monthly climatology of DMS flux by Lana et al. (2011) are further

https://doi.org/10.5194/egusphere-2025-1622
Preprint. Discussion started: 19 May 2025

adopted. To validate the modelling results of atmospheric DMS, we compare the simulated atmospheric DMS mixing ratio with previous measurements, especially for those at high altitudes. To date, historical data on atmospheric DMS mixing ratio at high altitudes over the SO is only available from HIAPER Pole-to-Pole Observations (HIPPO project) near the oceans of New Zealand (see more information from the website: https://www.eol.ucar.edu/field_projects/hippo). The simulated DMS mixing ratio based on Lana's emission near New Zealand is comparable with HIPPO's (Figure S4). The patterns of atmospheric DMS distribution agree well with each other at altitudes above approximately 2 km. For those data below 2 km (mostly located in MBL), the simulation results are generally higher than HIPPO's with the mean simulated values lying between the observed values range. Near the surface ocean, our simulated value of around 250 pptv is consistent with the measurement during CHINARE 34th (mean value was 260 ± 410 ppbv) (Zhang et al. 2019). Generally, our simulation of atmospheric DMS is reliable and can be used as an approximation of the real field values over the SO.

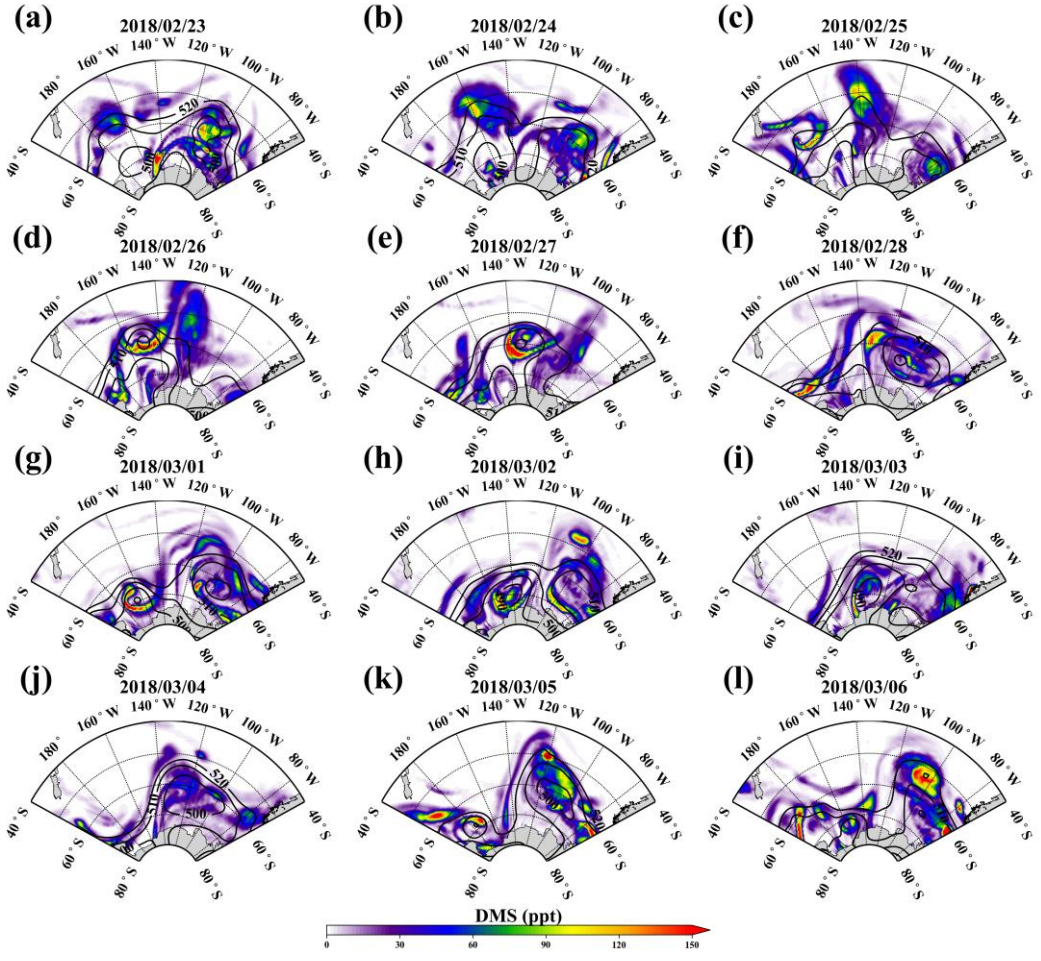

Figure 3, the daily simulation results of the distribution of atmospheric DMS at 5 km using Lana's emission climatology. a - l) the results of different investigation periods. Note that the mean 500 hPa geopotential air pressures are presented in the background.

https://doi.org/10.5194/egusphere-2025-1622
Preprint. Discussion started: 19 May 2025

The daily and mean simulation results at 5 km based on Lana's DMS emissions are shown in Figure 3 (see also Figure S5-S6 for the daily results at 1 km and 3 km, respectively). As expected, the simulated atmospheric DMS mixing ratios at different altitudes based on Lana's emissions are approximately two orders of magnitude higher than those based on the campaign data. Similarly, the low-pressure systems are also found to favor the vertical transport of DMS (Figure 3, S5-S6). Low-pressure systems induce wind convergence at lower altitudes, resulting in upward motion due to mass continuity, which would bring the DMS upward. For those results at 5 km altitude, the atmospheric DMS mixing ratio could reach up to 100 pptv (Figure 3), which is comparable with those records in the MBL over the tropical or subtropical ocean (e.g. 76.2 ± 52.2 pptv in the west Pacific Ocean, see in (Marandino et al. 2013)). It is also noteworthy that the DMS mixing ratio is generally higher behind (west side) rather than in front (east side) of the low-pressure, especially for the cyclones (e.g. Figure 3 e, g, l). This phenomenon might be due to northerly warm air flow in front of the low-pressure system, which may potentially act as a lid (temperature inversion) to suppress vertical mixing.

3.3 Cyclone enhances the contributions of oceanic DMS to the free troposphere over the SO and its implications

It is difficult for DMS to form aerosol particles large enough to act as CCN by homogeneous gas phase processes in MBL due to the relatively long reactive time (3-4 days) (Raes 1995). Some studies argued that DMS could condense on the surface of existing aerosols with small particle size, so that they grow and are activated as CCN, then increase the number of CCN (Quinn et al. 2017). However, reports showed that sea salt particles have enough size as the primary nuclei to form CCN in MBL in the SO area (Quinn and Bates 2011). Compared with MBL, DMS in FT could transform into H_2SO_4, and nucleation always and immediately takes place because of the cold temperatures and the low level of preexisting aerosols as they are partly removed by precipitation in the convective clouds, and then grow and become large enough to act as CCN when they mix into MBL (Raes 1995). Therefore, the DMS-derived new particles in the free troposphere but not in MBL could explain a significant source of MBL CCN from the entrainment of particles. It is also of interest to estimate the whole amount of atmospheric DMS transported to high altitudes.

An estimation based on the FLEXPART simulation is shown in Figure 4. As discussed above, the mixing height over the SO is commonly below 1.25 km (Figure 1 d). Therefore, we assume a height of 2 km to distinguish the boundary of the free troposphere and MBL in the estimation (Williamson et al. 2019). Generally, most of the oceanic DMS, approximately 91.4% and 86.9% of the original oceanic emitted DMS from the simulations based on CHINARE and Lana's data, respectively, is located below 2 km. But there is still a non-negligible fraction of oceanic DMS, about 8.6% (0.02 Gg) and 13.1% (127.66 Gg) calculated from the CHINARE and Lana's data respectively, transported to the free troposphere. Compared to the regions with strong vertical convection (e.g. the tropical and sub-tropical western Pacific Ocean, where approximately 30% of emitted oceanic DMS could leave the MBL (Marandino et al. 2013)), our simulation results are lower. However, the much higher DMS emission over the SO (Lana et al. 2011) is enough to provide a large amount (3.93 kg/km^2) of oceanic DMS into the free

https://doi.org/10.5194/egusphere-2025-1622
Preprint. Discussion started: 19 May 2025

troposphere, which is much higher than that in the western Pacific Ocean (8.3×10^{-5} to 1.7×10^{-4} kg/km^2) (Marandino et al. 2013).

Additionally, the DMS lifetime in the cold regions of high latitudes is possibly more prolonged than that in warmer regions of low latitude (Leck and Persson 1996; Read et al. 2008), suggesting that a much longer distance during the atmospheric transport process over the SO. It is also necessary to note that our simulation period is almost in the austral fall season, when the DMS emission in this period is much lower than that in the spring and summer with phytoplankton blooms (Lana et al. 2011). Therefore, a significant amount of DMS is expected to be transported to the free troposphere as the annual DMS emission over the SO accounts for approximately 20% (5.8 Tg S a^{-1}) of the global ocean (Lana et al. 2011).

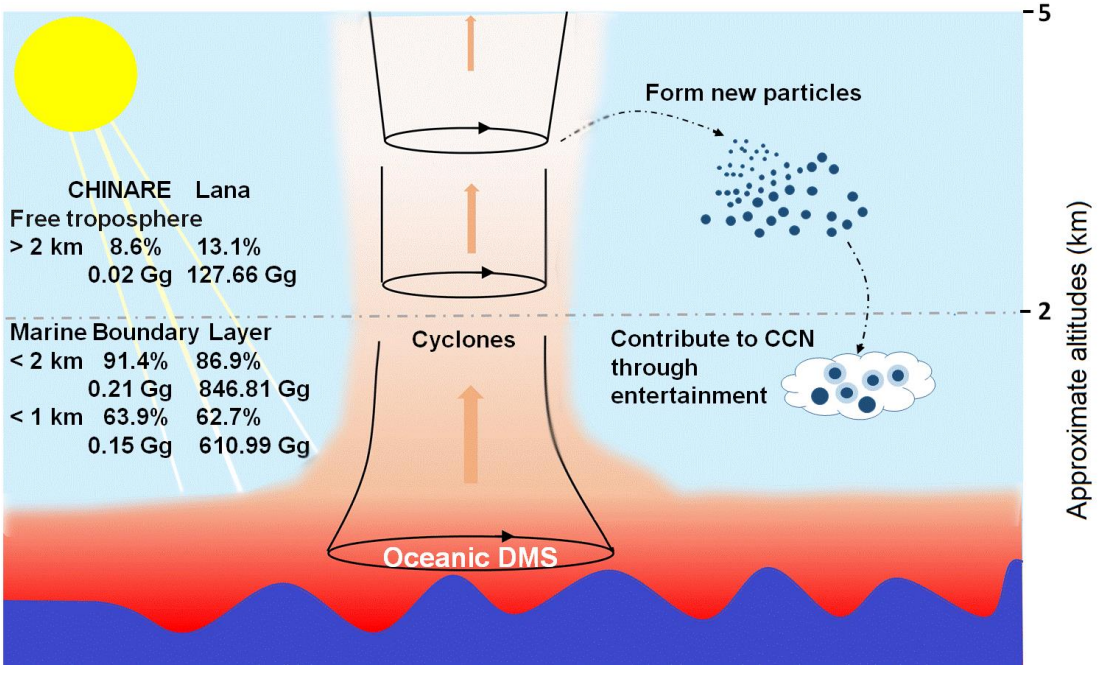

Figure 4. An estimation of oceanic DMS amount transported to the free troposphere and marine boundary layer (MBL) over the Southern Ocean from Feb 18 to Mar 10, 2018. The percentage and amount of DMS at different altitudes are presented on the left-hand side. The background is the schematic indicating the vertical transportation of oceanic DMS can be enhanced by the low-pressure system, e.g. cyclones, and the importance of DMS in forming new particles in the free troposphere, which could contribute to the CCN in MBL through entertainment. The red color shade indicated the DMS in the atmosphere.

It was reported that the new particle formation in coastal Antarctica is driven by ion-induced sulfuric acid-ammonia nucleation (Jokinen et al. 2018), suggesting that the oceanic DMS and its subsequent atmospheric oxidants, like sulfuric acid (H_2SO_4) and methane sulfonic acid (MSA), play an important role in controlling this process (O'Dowd et al. 1997). In fact,

https://doi.org/10.5194/egusphere-2025-1622
Preprint. Discussion started: 19 May 2025

under a clean and cold atmosphere, DMS can contribute to CCN through homogeneous nucleation by forming H_2SO_4 via a gas-phase oxidation route, instead of contributing to particle growth in the MBL (Woodhouse et al. 2013). Therefore, new particle formation is expected to occur in a similar clean and cold-free troposphere if abundant oceanic DMS could be transported to this altitude. The relatively high DMS mixing ratio (> 100 pptv at an altitude of 5 km, Figure 3), in the free troposphere surrounding the low-pressure cores or troughs in our simulation, is likely to favor the large production of new particles over the high altitudes of SO.

In contrast, in the tropical convective oceans, a large source of CCN from new particle formation caused by the detrainment of gases has been investigated (Williamson et al. 2019), and the subsidence and entrainment of free troposphere particles strongly influenced the MBL CCN populations in those tropical oceans (Clarke et al. 2013). Due to the limited measurement of new particle formation over the high altitude of SO, it is not enough to test and verify the phenomenon. However, the DMS-derived new particles in the free troposphere could explain a significant source of MBL CCN from the entrainment of particles (Quinn et al. 2017). The coincidence patterns between the relatively high DMS levels at high altitudes and low-pressure cores or troughs also suggest that the low-pressure system possibly facilitates the new particle formation in the free troposphere (Figure 3). Thus, to fully understand the influence of oceanic DMS on the CCN population, further studies about quantifying the fraction of CCN in the MBL caused by the entrainment of DMS-derived particles in the free troposphere are also necessary over the SO.

4.0 Summary

In the present study, we deploy FLEXPART to simulate the atmospheric transport of oceanic DMS emitted to the atmosphere based on the DMS emission data from the CHINARE campaign and Lana's climatology from Feb 18, 2018, to Mar 10, 2018. As the SO is a huge source of marine DMS (Lana et al. 2011), our modelling results indicated that significant oceanic DMS, about 8.6% and 13.1% of the originally emitted DMS from CHINARE and Lana's data respectively, could be transported to the altitudes above 2 km. The vertical transportation of oceanic DMS is enhanced by the low-pressure systems. Relatively high DMS mixing ratios, up to above 100 pptv at an altitude of 5 km, are found surrounding the low-pressure cores or troughs from Lana's DMS emission climatology over the SO. These results suggested that a large DMS-derived new particle formation is expected over the SO-free troposphere, and thus, those particles might act as a vital source of MBL CCN over the SO through subsidence and entrainment of free troposphere particles.

Code Availability

The code used in this study is available from the corresponding author upon request.

https://doi.org/10.5194/egusphere-2025-1622
Preprint. Discussion started: 19 May 2025

Data Availability

All the data we used in this manuscript was upload to a online database https://figshare.com. The DOI information of the data is https://doi.org/10.6084/m9.figshare.28806161.v1. The data could be download freely from this website.

Author contributions

Dr. Miming Zhang and Dr. Yue Jia contributed equally to this study. Dr. Miming Zhang wrote the manuscript and Dr. Yue Jia ran the model. The other authors joined the discussion and revision of this manuscript.

Acknowledgements

We thank the Chinese Arctic and Antarctic Administration (CAA) of the Ministry of Natural Resources and the crew of R/V *Xue Long* for their support with field operations. Our datasets are currently included in the Supporting Information and will be uploaded to the PANGAEA repository after publication. This work was financially supported by the National Natural Science Foundation of China (NSFC) (42076226, 42476253), the China Scholarship Council (CSC No. 202304180025). This study was also supported by Cultivating Innovation Team Program of Third Institute of Oceanography.

Competing Interests

The authors declare they have no competing interests.

Supplementary information

Figure S1. The daily simulation results of the distribution of atmospheric DMS at 1 km using the CHINARE's campaign DMS emission

Figure S2. The daily simulation results of the distribution of atmospheric DMS at 3 km using the CHINARE's campaign DMS emission.

Figure S3. The daily simulation results of the distribution of atmospheric DMS at 5 km using the CHINARE's campaign DMS emission.

Figure S4. The comparison of the modelling results of mean DMS mixing ratio using the Lana's climatology near the ocean of New Zealand and HIPPO flight measurement data.

Figure S5. The daily simulation results of the distribution of atmospheric DMS at 1km using Lana's emission climatology

Figure S6. The daily simulation results of the distribution of atmospheric DMS at 3 km using Lana's emission climatology

https://doi.org/10.5194/egusphere-2025-1622
Preprint. Discussion started: 19 May 2025

References

Ayers, GP, and RW Gillett. DMS and its oxidation products in the remote marine atmosphere: implications for climate and atmospheric chemistry, Journal of Sea Research, 43: 275-86. 2000.

Charlson, R.J., J.E. Lovelock, M.O. Andreaei, and S.G. Warren.. Oceanic phytoplankton, atmospheric sulphur, cloud, Nature, 326: 655-61. 1987

Clarke, A. D., S. Freitag, R. M. C. Simpson, J. G. Hudson, S. G. Howell, V. L. Brekhovskikh, T. Campos, V. N. Kapustin, and J. Zhou.Free troposphere as a major source of CCN for the equatorial pacific boundary layer: long-range transport and teleconnections, Atmospheric. Chemistry and. Physics., 13: 7511-29. 2013.

Curran, Mark A. J., Graham B. Jones, and Harry Burton. Spatial distribution of dimethylsulfide and dimethylsulfoniopropionate in the Australasian sector of the Southern Ocean, Journal of Geophysical. Research., 103: 16677-89. 1998.

Dacey, John W. H., Stuart G. Wakeham, and Brian L. Howes. Henry's law constants for dimethylsulfide in freshwater and seawater, Geophysical Research Letters, 11: 991-94. 1984.

Dee, D. P., S. M. Uppala, A. J. Simmons, P. Berrisford, P. Poli, S. Kobayashi, U. Andrae, M. A. Balmaseda, G. Balsamo, P. Bauer, P. Bechtold, A. C. M. Beljaars, L. van de Berg, J. Bidlot, N. Bormann, C. Delsol, R. Dragani, M. Fuentes, A. J. Geer, L. Haimberger, S. B. Healy, H. Hersbach, E. V. Hólm, L. Isaksen, P. Kållberg, M. Köhler, M. Matricardi, A. P. McNally, B. M. Monge-Sanz, J.-J. Morcrette, B.-K. Park, C. Peubey, P. de Rosnay, C. Tavolato, J.-N. Thépaut, and F. Vitart.. The ERA-Interim reanalysis: configuration and performance of the data assimilation system, Quarterly Journal of the Royal Meteorological Society, 137: 553-97. 2011

Dusek, Ulrike, GP Frank, Lea Hildebrandt, Joachim Curtius, Johannes Schneider, Saskia Walter, Duli Chand, Frank Drewnick, Silke Hings, and D Jung. Size matters more than chemistry for cloud-nucleating ability of aerosol particles, Science, 312: 1375-78. 2006.

Emanuel, Kerry A., and Marina Živković-Rothman. Development and Evaluation of a Convection Scheme for Use in Climate Models, Journal of the Atmospheric Sciences, 56: 1766-82. 1999.

Forster, Caroline, Andreas Stohl, and Petra Seibert. Parameterization of Convective Transport in a Lagrangian Particle Dispersion Model and Its Evaluation, Journal of Applied Meteorology and Climatology, 46: 403-22. 2007.

Gabric, Albert J., Jill M. Shephard, Jon M. Knight, Graham Jones, and Anne J. Trevena. Correlations between the satellite-derived seasonal cycles of phytoplankton biomass and aerosol optical depth in the Southern Ocean: Evidence for the influence of sea ice, Global Biogeochemical Cycles, 19: GB4018. 2005.

Inomata, Yayoi, Masahiko Hayashi, Kazuo Osada, and Yasunobu Iwasaka. Spatial distributions of volatile sulfur compounds in surface seawater and overlying atmosphere in the northwestern Pacific Ocean, eastern Indian Ocean, and Southern Ocean , Global Biogeochem. Cycles, 20: GB2022. 2006.

Irving, Damien, Ian Simmonds, and Kevin Keay. Mesoscale Cyclone Activity over the Ice-Free Southern Ocean: 1999–2008 ,

https://doi.org/10.5194/egusphere-2025-1622
Preprint. Discussion started: 19 May 2025

Journal of Climate, 23: 5404-20. 2010.

Jokinen, T., M. Sipilä, J. Kontkanen, V. Vakkari, P. Tisler, E.-M. Duplissy, H. Junninen, J. Kangasluoma, H. E. Manninen, T. Petäjä, M. Kulmala, D. R. Worsnop, J. Kirkby, A. Virkkula, and V.-M. Kerminen. Ion-induced sulfuric acid–ammonia nucleation drives particle formation in coastal Antarctica , Science Advances, 4: eaat9744. 2018.

Kettle, AJ, MO Andreae, D. Amouroux, TW Andreae, TS Bates, H. Berresheim, H. Bingemer, R. Boniforti, MAJ Curran, and GR DiTullio. A global database of sea surface dimethylsulfide (DMS) measurements and a procedure to predict sea surface DMS as a function of latitude, longitude, and month , Global Biogeochemical Cycles, 13: 399-444. 1999.

Kim, I, D Hahm, K Park, Y Lee, J. O. Choi, M. Zhang, L. Chen, H. C. Kim, and S Lee. Characteristics of the horizontal and vertical distributions of dimethyl sulfide throughout the Amundsen Sea Polynya , Science of the Total Environment, 584-585: 154. 2017.

Lana, Arantxa, TG Bell, Rafel Simó, Sergio M Vallina, Joaquim Ballabrera-Poy, AJ Kettle, Jordi Dachs, L Bopp, ES Saltzman, and J Stefels. An updated climatology of surface dimethlysulfide concentrations and emission fluxes in the global ocean , Global Biogeochemical Cycles, 25: GB1004. 2011.

Leck, Caroline, and Cecilia Persson. Seasonal and short-term variability in dimethyl sulfide, sulfur dioxide and biogenic sulfur and sea salt aerosol particles in the arctic marine boundary layer during summer and autumn , Tellus B, 48: 272-99. 1996.

Liss, Peter S, Christa A Marandino, Elizabeth E Dahl, Detlev Helmig, Eric J Hintsa, Claire Hughes, Martin T Johnson, Robert M Moore, John MC Plane, and Birgit Quack. Short-lived trace gases in the surface ocean and the atmosphere. in, Ocean-Atmosphere Interactions of Gases and Particles (Springer). 2014.

Marandino, CA, Susann Tegtmeier, Kirstin Krüger, Cathleen Zindler, EL Atlas, F Moore, and Hermann W Bange. Dimethylsulphide (DMS) emissions from the western Pacific Ocean: a potential marine source for stratospheric sulphur? , Atmospheric Chemistry and Physics, 13: 8427-37. 2013.

McCoy, Daniel T., Susannah M. Burrows, Robert Wood, Daniel P. Grosvenor, Scott M. Elliott, Po-Lun Ma, Phillip J. Rasch, and Dennis L. Hartmann. Natural aerosols explain seasonal and spatial patterns of Southern Ocean cloud albedo , Science Advances, 1: e1500157. 2015.

McGillis, WR, JWH Dacey, NM Frew, EJ Bock, and RK Nelson. Water-air flux of dimethylsulfide , Journal of Geophysical Research, 105: 1187-93. 2000.

Merikanto, J., D. V. Spracklen, G. W. Mann, S. J. Pickering, and K. S. Carslaw. Impact of nucleation on global CCN , Atmospheric Chemistry and Physics., 9: 8601-16. 2009.

Murphy, DM, JR Anderson, PK Quinn, LM McInnes, FJ Brechtel, SM Kreidenweis, AM Middlebrook, M. Posfai, DS Thomson, and PR Buseck. Influence of sea-salt on aerosol radiative properties in the Southern Ocean marine boundary layer , Nature, 392: 62-65. 1998.

Nightingale, P.D., G. Malin, C.S. Law, A.J. Watson, P.S. Liss, M.I. Liddicoat, J. Boutin, and R.C. Upstill-Goddard. In situ evaluation of air-sea gas exchange parameterizations using novel conservative and volatile tracers , Global

https://doi.org/10.5194/egusphere-2025-1622
Preprint. Discussion started: 19 May 2025

Biogeochem. Cycles, 14: 373-87. 2000.

O Dowd, Colin D, Jason A Lowe, Michael H Smith, Brian Davison, C Nicholas Hewitt, and Roy M Harrison. Biogenic sulphur emissions and inferred non-sea-salt-sulphate cloud condensation nuclei in and around Antarctica , Journal of Geophysical Research: Atmospheres (1984–2012), 102: 12839-54. 1997.

Park, Ki-Tae, Young Jun Yoon, Kitack Lee, Peter Tunved, Radovan Krejci, Johan Ström, Eunho Jang, Hyo Jin Kang, Sehyun Jang, Jiyeon Park, Bang Yong Lee, Rita Traversi, Silvia Becagli, and Ove Hermansen. Dimethyl Sulfide-Induced Increase in Cloud Condensation Nuclei in the Arctic Atmosphere , Global Biogeochemical Cycles, 35: e2021GB006969. 2021.

Patoux, Jérôme, Xiaojun Yuan, and Cuihua Li. Satellite-based midlatitude cyclone statistics over the Southern Ocean: 1. Scatterometer-derived pressure fields and storm tracking , Journal of Geophysical Research: Atmospheres, 114. 2009.

Plessis, Marcel du, Sebastiaan Swart, Isabelle J. Ansorge, Amala Mahadevan, and Andrew F. Thompson. Southern Ocean Seasonal Restratification Delayed by Submesoscale Wind–Front Interactions , Journal of Physical Oceanography, 49: 1035-53. 2019.

Quinn, P. K., D. J. Coffman, J. E. Johnson, L. M. Upchurch, and T. S. Bates. Small fraction of marine cloud condensation nuclei made up of sea spray aerosol , Nature Geoscience, 10: 674. 2017.

Quinn, PK, and TS Bates. The case against climate regulation via oceanic phytoplankton sulphur emissions , Nature, 480: 51-56. 2011.

Quinn, PK, DJ Coffman, VN Kapustin, TS Bates, and DS Covert. Aerosol optical properties in the marine boundary layer during the First Aerosol Characterization Experiment (ACE 1) and the underlying chemical and physical aerosol properties , Journal of Geophysical Research: Atmospheres, 103: 16547-63. 1998.

Raes, Frank. Entrainment of free tropospheric aerosols as a regulating mechanism for cloud condensation nuclei in the remote marine boundary layer , Journal of Geophysical Research: Atmospheres, 100: 2893-903. 1995.

Read, KA, AC Lewis, Stephane Bauguitte, Andrew M Rankin, RA Salmon, Eric W Wolff, A Saiz-Lopez, WJ Bloss, DE Heard, and JD Lee. DMS and MSA measurements in the Antarctic Boundary Layer: impact of BrO on MSA production , Atmospheric Chemistry and Physics, 8: 2985-97. 2008.

Rosenfeld, Daniel, Steven Sherwood, Robert Wood, and Leo Donner. Climate effects of aerosol-cloud interactions , Science, 343: 379-80. 2014.

Sanchez, Kevin J., Chia-Li Chen, Lynn M. Russell, Raghu Betha, Jun Liu, Derek J. Price, Paola Massoli, Luke D. Ziemba, Ewan C. Crosbie, Richard H. Moore, Markus Müller, Sven A. Schiller, Armin Wisthaler, Alex K. Y. Lee, Patricia K. Quinn, Timothy S. Bates, Jack Porter, Thomas G. Bell, Eric S. Saltzman, Robert D. Vaillancourt, and Mike J. Behrenfeld. Substantial Seasonal Contribution of Observed Biogenic Sulfate Particles to Cloud Condensation Nuclei , Scientific Reports, 8: 3235. 2018.

Simpson, Rebecca M. C., Steven G. Howell, Byron W. Blomquist, Antony D. Clarke, and Barry J. Huebert. Dimethyl sulfide: Less important than long-range transport as a source of sulfate to the remote tropical Pacific marine boundary layer ,

https://doi.org/10.5194/egusphere-2025-1622
Preprint. Discussion started: 19 May 2025

Journal of Geophysical Research: Atmospheres, 119: 9142-67. 2014.

Stohl, A., C. Forster, A. Frank, P. Seibert, and G. Wotawa. Technical note: The Lagrangian particle dispersion model FLEXPART version 6.2 , Atmos. Chem. Phys., 5: 2461-74. 2005.

Stohl, A., M. Hittenberger, and G. Wotawa. Validation of the lagrangian particle dispersion model FLEXPART against large-scale tracer experiment data , Atmospheric Environment, 32: 4245-64. 1998.

Stohl, Andreas, and David J. Thomson. A Density Correction for Lagrangian Particle Dispersion Models , Boundary-Layer Meteorology, 90: 155-67. 1999.

Stohl, Andreas, and Thomas Trickl. A textbook example of long-range transport: Simultaneous observation of ozone maxima of stratospheric and North American origin in the free troposphere over Europe , Journal of Geophysical Research: Atmospheres, 104: 30445-62. 1999.

Tegtmeier, Susann, Kirstin Krüger, Birgit Quack, E Atlas, DR Blake, H Boenisch, A Engel, Helmke Hepach, R Hossaini, and MA Navarro. The contribution of oceanic methyl iodide to stratospheric iodine , Atmospheric Chemistry and Physics, 13: 11869-86. 2013.

Tortell, P.D., and M.C. Long. Spatial and temporal variability of biogenic gases during the Southern Ocean spring bloom , Geophysical Research Letters, 36: L01603. 2009.

Tortell, P.D., M.C. Long, C.D. Payne, A.C. Alderkamp, P. Dutrieux, and K.R. Arrigo. Spatial distribution of pCO_2, $\Delta O_2/Ar$ and dimethylsulfide (DMS) in polynya waters and the sea ice zone of the Amundsen Sea, Antarctica , Deep Sea Research Part II: Topical Studies in Oceanography, 71-76: 77-93. 2012.

Tortell, PD, C. Gueguen, MC Long, CD Payne, P. Lee, and GR DiTullio. Spatial variability and temporal dynamics of surface water pCO_2, $\Delta O_2/Ar$ and dimethylsulfide in the Ross Sea, Antarctica , Deep Sea Research Part I: Oceanographic Research Papers, 58: 241-59. 2011.

Vallina, S. M., R. Simó, and S. Gassó. What controls CCN seasonality in the Southern Ocean? A statistical analysis based on satellite-derived chlorophyll and CCN and model-estimated OH radical and rainfall , Global Biogeochemical Cycles, 20: GB1014. 2006.

Williamson, Christina J., Agnieszka Kupc, Duncan Axisa, Kelsey R. Bilsback, ThaoPaul Bui, Pedro Campuzano-Jost, Maximilian Dollner, Karl D. Froyd, Anna L. Hodshire, Jose L. Jimenez, John K. Kodros, Gan Luo, Daniel M. Murphy, Benjamin A. Nault, Eric A. Ray, Bernadett Weinzierl, James C. Wilson, Fangqun Yu, Pengfei Yu, Jeffrey R. Pierce, and Charles A. Brock. A large source of cloud condensation nuclei from new particle formation in the tropics , Nature, 574: 399-403. 2019.

Woodhouse, MT, GW Mann, KS Carslaw, and O Boucher. Sensitivity of cloud condensation nuclei to regional changes in dimethyl-sulphide emissions , Atmospheric Chemistry and Physics, 13: 2723-33. 2013.

Yuan, Xiaojun, Jérôme Patoux, and Cuihua Li. Satellite-based midlatitude cyclone statistics over the Southern Ocean: 2. Tracks and surface fluxes , Journal of Geophysical Research: Atmospheres, 114. 2009.

Zhang, Miming, Wei Gao, Jinpei Yan, Yanfang Wu, Christa A. Marandino, Keyhong Park, Liqi Chen, Qi Lin, Guobin Tan, and

https://doi.org/10.5194/egusphere-2025-1622
Preprint. Discussion started: 19 May 2025

Meijiao Pan. An integrated sampler for shipboard underway measurement of dimethyl sulfide in surface seawater and air , Atmospheric Environment, 209: 86-91. 2019.

Zhang, Miming, C. A. Marandino, Liqi Chen, Heng Sun, Zhongyong Gao, Keyhong Park, Intae Kim, Bo Yang, Tingting Zhu, Jinpei Yan, and Jianjun Wang. Characteristics of the surface water DMS and pCO_2 distributions and their relationships in the Southern Ocean, southeast Indian Ocean, and northwest Pacific Ocean , Global Biogeochemical Cycles, 31: 1318-31. 2017.

Zhang, Miming, Ki-Tae Park, Jinpei Yan, Keyhong Park, Yanfang Wu, Eunho Jang, Wei Gao, Guobin Tan, Jianjun Wang, and Liqi Chen. Atmospheric dimethyl sulfide and its significant influence on the sea-to-air flux calculation over the Southern Ocean , Progress in Oceanography, 186: 102392. 2020.